drothermal venting and associated metalliferous deposits should be sought all along the East Pacific Rise. The 13°N area differs morphologically from the 21°N area, where the spreading rate is about half as fast. It will now be important to establish the distribution of hydrothermal activity between fracture zones. We briefly investigated a second area of the axial zone (zone B, near 11°30′N) along the rise segment between the Orozco and Clipperton fracture zones and found indications of hydrothermal activity from hydrocasts and sea-floor photographs. Finally, the presence of massive sulfides on off-axis seamounts opens an interesting field for further exploration.

R. HEKINIAN
Centre Océanologique de Bretagne, 29273 Brest Cédex, France
M. FEVRIER
Centre Océanologique de Bretagne and *Département de Géologie, Université de Bretagne Occidentale, 29283 Brest Cédex, France*
F. AVEDIK
P. CAMBON
J. L. CHARLOU
H. D. NEEDHAM
J. RAILLARD
Centre Océanologique de Bretagne
J. BOULEGUE
Université de Paris 6 et 7, 75230 Paris Cédex 05, France
L. MERLIVAT
DPC-CEN Saclay, 91191 Gif-sur-Yvette Cédex, France
A. MOINET
Université de Paris 6 et 7
S. MANGANINI
Woods Hole Oceanographic Institution, Woods Hole, Massachusetts 02543
J. LANGE
Preussag Aktiengesellschaft, 3000 Hannover, Federal Republic of Germany

References and Notes

1. Cyamex Scientific Team, *Mar. Geophys. Res.* **4**, 345 (1981).
2. RISE Project Group, *Science* **207**, 1421 (1980).
3. R. L. Larson, *Bull. Geol. Am.* **82**, 823 (1971).
4. Cyamex Scientific Team and H. Bougault, P. Cambon, R. Hekinian, *Nature (London)* **277**, 5601 (1979).
5. L. Merlivat, J. Boulegue, B. Dimon, *Eos* **62**, 913 (1981).
6. J. Francheteau, abstract of paper presented at the American Geophysical Union Chapman Conference, Warrenton, Va., 1981.
7. R. D. Ballard, J. Francheteau, T. Juteau, C. Rangin, W. Normark, *Earth Planet. Sci. Lett.* **55**, 1 (1981).
8. R. D. Ballard, R. T. Holcomb, T. H. Van Andel, *J. Geophys. Res.* **84**, 5407 (1979).
9. M. Fevrier, thesis, Université de Bretagne Occidentale and Centre Océanologique de Bretagne, Brest, France (1981).
10. M. M. Styrt *et al.*, *Earth Planet. Sci. Lett.* **53**, 382 (1981).
11. R. M. Haymon and M. Kastner, *ibid.*, p. 363.
12. S. Honjo and J. F. Cannell, *Woods Hole Oceanogr. Inst. Tech. Rep. WHOI-79-80* (1979).
13. The Clipperton cruise was carried out as part of the CNEXO program for the study of ocean floor hydrothermalism. We are grateful to Captain G. Paquet and the officers and crew of the R.V. *Jean Charcot* for the skillful handling of the wide range of equipment used during the cruise. We thank J. Legrand, M. Lehaitre, and G. Vincent for operating the deep-towed camera system RAIE; J. C. Cavarec for handling the bottom-moored transponder navigational system; and J. L. Reaute, A. Le Bot, and A. Gourmelon for acquisition of the multichannel narrow-beam echo sounder (Seabeam) data. R. Conogan and J. Roudaut assisted in handling the seismic reflection gear. G. Floch was responsible for the rock inventory and thin sections on board. Final maps were prepared by D. Carre, A. Grotte, and S. Monti. M. Bohn performed the microprobe analysis of the samples and S. Marques and R. Kerbrat screened the sediment samples for examination and chemical analysis.

19 July 1982; revised 16 November 1982

Controlled Stimulation of Magnetospheric Electrons by Radio Waves: Experimental Model for Lightning Effects

Abstract. *Magnetospheric electrons precipitated by ground-based coded very low frequency radio transmissions have been detected by rocket measurement of bremsstrahlung x-rays, caused by impact of the electrons with the upper atmosphere. The direct correlations obtained between the very low frequency signals and the x-rays demonstrate the limits of sensitivity required and indicate that this remote sensing technique would be useful for future study of very low frequency effects induced by single lightning strokes.*

Recent interest in influences of human activities on the upper terrestrial environment has centered on radio wave stimulation of plasma-wave instabilities in the magnetosphere (*1*). The magnetosphere is the outermost portion of the near-earth environment and is regulated by interaction between the earth's and interplanetary plasmas and magnetic fields. Two principal anthropogenic sources of radio wave noise are thought to arise from power lines (*2*) and high-powered very low frequency (VLF) transmitters (*3, 4*), although serious doubts have been raised about the magnitude of the effect from power lines (*5*). Theoretical studies (*4, 6*) imply that the radio waves should trigger the precipitation of energetic electrons from the trapped particle belts in the earth's magnetosphere.

Before now, direct experimental verification of the occurrence of transmitter-induced electron precipitation has not been obtained (*4*). Indirect evidence has been offered in the form of narrow peaks observed in the energy spectra of precipitating electrons linked with VLF transmitter signals (*7*), satellite-based observations of emission triggering by VLF transmitters (*8*), and low-latitude energetic (> 100 keV) electron precipitation linked to Soviet transmitters (*9*). In addition, fluctuations in ground-based riometer records have been attributed to ionospheric modulations caused by VLF-induced electron precipitation from Siple Station, Antarctica (*10*), and perturbations in propagating signals from transmitters in the Northern Hemisphere have been linked to enhanced ionization from electron precipitation at the ends of field lines (*11*). This indirect evidence combined with recent theoretical results provided the motivation for the experiment described here. Finally, it should be noted that for natural VLF sources, possible correlations between particle

Table 1. Rocket flight and range logistics.

Datum	Rocket 31.030	Rocket 31.031
	Time	
Date	23 June 1982	7 July 1982
Launch (T_0)	1540 UT (day)	0901 UT (night)
Apogee	T_0 + 148.9 sec	T_0 + 144.9 sec
	Altitude	
Apogee	84.8 km	80.0 km
T_0 + 300 sec	49.4 km	48.1 km
T_0 + 540 sec	34.3 km	33.9 km
	Transmitter time	
On	1539 UT	0900 UT
Off	1549 UT	0910 UT
	Range coordinates	
Position	37.9°N, 75.5°W	37.9°N, 75.5°W
Magnetic L value	2.60	2.60
	Transmitter coordinates	
Position	39.0°N, 76.5°W	39.0°N, 76.5°W
Magnetic L value	2.76	2.74

precipitation bursts and lightning-induced VLF waves have also been reported (*12*).

In the past few months, the dedicated satellite SEEP (stimulated emission of energetic particles) (*13*) and two rockets have been launched to detect electron emissions induced by coded monofrequency VLF signals transmitted by high-powered ground-based stations in North America. Here we describe preliminary results from two Nike-Orion rocket flights launched from Wallops Island, Virginia, on 23 June (1540 UT, daytime) and 7 July (0901 UT, nighttime) 1982. The launches were conducted in conjunction with transmitted signals from the NSS transmitter at Annapolis, Maryland. During each rocket flight and for a duration of 10 minutes, the 0.25-MW continuous-wave (CW) signals were radiated at 21.4 kHz with a duty cycle of 3 seconds on followed by 2 seconds off. The rocket payloads each separated with nose cone and parachute deployment near apogee, to permit a stable platform with slow descent during the data acquisition period. The rocket flight and range logistics are given in Table 1. The 23 June rocket flight was coordinated with a SEEP overpass; the results are not compared here. However, the SEEP data have been partially examined and appear consistent with our results and hypotheses (*14*).

For this experiment, each rocket payload included a zenith-viewing NaI scintillation x-ray detector with five integral energy channels at thresholds of 5, 10, 20, 40, and 80 keV. Also included were a Geiger tube electron detector (> 40 keV), a VLF receiver, and a two-axis magnetometer to measure platform stability.

The x-ray detector was provided to monitor bremsstrahlung x-rays, caused by impact of energetic electrons with the upper atmosphere. X-rays penetrate to much lower atmospheric depths than do the parent electrons. Thus, by remotely sensing the electron fluxes through the emitted x-ray radiation with a wide-angle detector having a geometric factor of about 4.5 cm^2-sr (solid angle, ~ 1 sr), it is possible to integrate the electron flux over a large area and for the full period of the VLF transmission. Furthermore, since the anticipated precipitating electron fluxes are nonuniform in space and time, an in situ particle detector would not yield a representative sample of the overall flux. The disadvantage in remote sensing with x-rays lies in the low efficiency (~ 10^{-4}) of the bremsstrahlung conversion process in the energy range of interest here.

Figure 1a is an example of the unprocessed data observed for the daytime (31.030) flight. Figure 1b is the corresponding example for the nighttime (31.031) flight. In this compressed time format, which projects to the termination of the coded VLF transmission, the x-ray count rates in the > 5 keV channel sampled every 2 msec are presented along with the received VLF signal in arbitrary units. Also shown is the flight trajectory. From this and other expanded plots in which both integral and differential count rates for the various channels are compared, no obvious correlation with the transmitted signal was found on either flight. This is due to the high contribution (> 80 percent) of cosmic-ray noise and, at higher altitudes, galactic x-ray noise to the count rates shown. However, a cross-correlation analysis given by

$$C(\tau) = \frac{1}{\Delta t} \int_{\Delta t} S(t)\, T\,(t - \tau)\, dt$$

showed a strong connection between the VLF transmitter signals and precipitating electron fluxes for the night launch. Here $C(\tau)$ is an unnormalized correlation coefficient, $S(t)$ is the x-ray signal, $T(t)$ is the pulsed VLF signal, t is time, Δt is the time interval for correlation, and τ is the delay time.

Idealized values of $C(\tau)$ for $S(t)$ and $T(t)$ having identical pulse shapes are shown in Fig. 2a (curve A). For comparison (curve B), $S(t)$ is also modeled as having a spikelike exponential rise near the end of the 3-second "on" pulse of the transmitter. For these cases $S(t)$ was a combination of the described signal pulse added to a randomly generated background noise to obtain a signal-to-noise ratio comparable to that in the experiment. These idealized curves represent the two limiting cases of strong scattering from the first second of the 3-second transmissions (curve A) and onset of scattering only near the end of each transmission (curve B).

For 31.030, plots of $C(\tau)$ against τ in increments of 0.1 second are presented in Fig. 2b, based on the integral count rate data for > 5 and > 10 keV and differential count rate data in the range 5

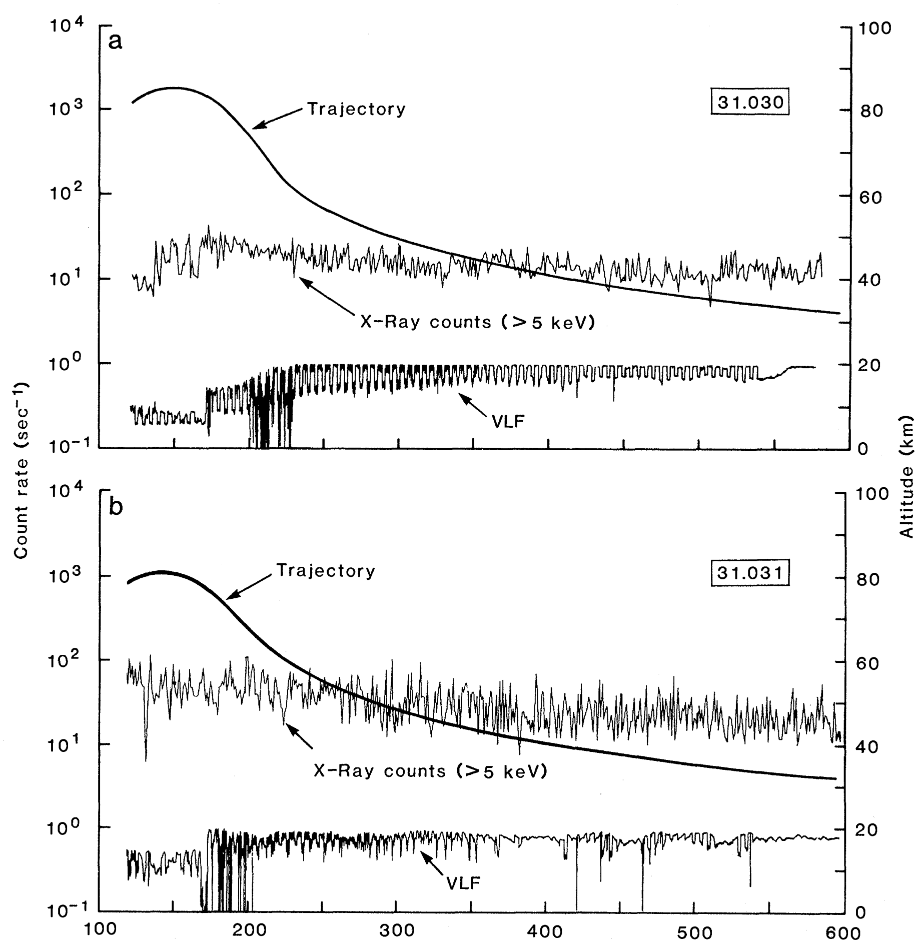

Fig. 1. X-ray count rates for electrons with energy > 5 keV as a function of time after rocket launch for (a) the day launch and (b) the night launch. Also shown are the trajectory altitude as a function of elapsed time and the VLF signal measured in arbitrary units by the onboard receiver. The rapid rise in VLF signal at approximately 170 seconds is due to the deployment of the VLF–electric field booms. The noise that occurs shortly after boom deployment stops as soon as the elective field antennas settle into place.

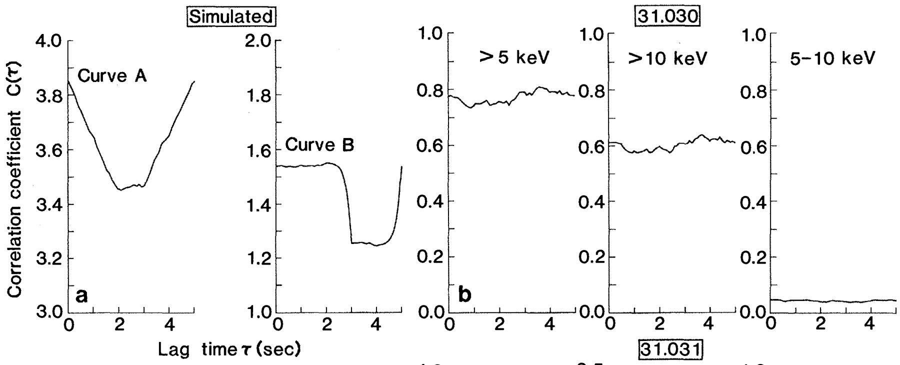

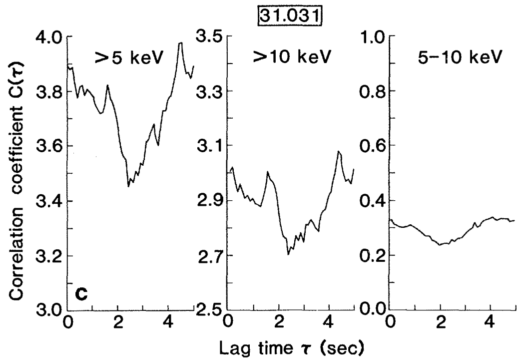

Fig. 2. Correlation curves as given by $C(\tau)$. (a) Simulated data generated by combining a random noise component with a transmitter correlated signal. Curve A was obtained by assuming that an x-ray signal existed whenever the transmitter was on. Curve B represents the case when the signal was exponentially turned on with an *e*-folding time of 0.2 second near the end of the transmitter pulse. The two cases are extrema for comparison with the data. If the signal and transmitter were not correlated, the curves would be flat except for random noise variations. (b) Correlation curves for day launch data for the integral channels > 5 and > 10 keV and the differential channel 5 to 10 keV from 150 to 300 seconds into the flight. (c) Correlation curves for night launch data for the same channels, also from 150 to 300 seconds into the flight.

to 10 keV. The flat $C(\tau)$ curve shows a null result, implying no measurable return signal in the x-ray data. The integration interval from 150 seconds (apogee) to 300 seconds (~ 50 km) in the two lowest energy channels limited the statistical analysis to a height domain where these lower energy x-rays are not excessively absorbed by the atmosphere. The higher energy data also showed no identifiable correlation.

The nighttime data (31.031) are illustrated for the same channels in Fig. 2c. The scattering that produces the precipitating particles is much stronger here, as evidenced by a triangular correlation pattern most closely resembling similar pulse shapes for $S(t)$ and $T(t)$—for instance, curve A in Fig. 2a. No identifiable correlation was observed above 20 keV. The clear signature of the correlation as high as the > 10 keV channel in Fig. 2c indicates the greatly enhanced precipitation under nighttime conditions. This is expected because the transmitted VLF signal is less heavily absorbed by the ionospheric D region under nighttime conditions, which increases the strength of the signal reaching the magnetosphere. Since the diffusion of the electrons into the atmospheric loss cone is proportional to the energy density of the VLF waves that enter the magnetosphere (*15*), enhanced precipitating fluxes are expected in nighttime. Furthermore, magnetic activity during the 12 hours preceding the nighttime flight was somewhat higher than for the daytime flight, which might have made more trapped electrons available for precipitation by increased filling of the radiation belts.

To check the results presented here, several cross-correlation tests were made with daytime and nighttime data for regions where no signal $S(t)$ would be expected. First, the low-energy x-rays (5 to 10 keV) were analyzed during the time period 300 to 540 seconds (payload altitude < 50 km) and produced the anticipated flat curve for $C(\tau)$ versus τ. Second, all channels were analyzed for the 10-minute period following transmitter shutdown from the coded mode, and the same null result was obtained. Finally, the nighttime data for the period 150 to 300 seconds were divided into two subintervals, each of which showed the similar triangular $C(\tau)$ pattern, but with poorer definition, as expected for shorter data sets.

We note that these nighttime data were subject to a payload radio interference problem, which increased the random noise level in the first two x-ray channels during the nighttime flight. This has prevented an absolute determination of the cross-correlation coefficient, although the shape of $C(\tau)$ and the arguments above remain valid because of the random nature of the noise signal. The noise also contributes in part to the higher count rates observed at night (Fig. 1).

The upper limits on energy for the x-ray flux (< 20 keV) can be equated to a similar limit for the parent electron flux because of the characteristics of the bremsstrahlung conversion process. For example, monoenergetic electron beams of energy E_0 typically produce relatively flat x-ray spectra for $0 < E < E_0$ (*16*).

Finally, the VLF data received on the nighttime launch have been analyzed and a nominal value of 10 W has been estimated for the transmitted VLF power illuminating the part of the lower magnetosphere observed by the x-ray detector during the experiment. Direct measurement of lightning transients in the ionosphere above a thunderstorm indicate broadband short-duration VLF power fluxes more than ten times as high as those estimated here for the transmitter (*17*). This suggests that lightning may make a significant contribution to the processes that stimulate electron precipitation in the magnetosphere. Furthermore, the contribution from single lightning strokes appears adequate to produce electron bursts in sufficient fluxes to be detected by sensors similar to those we used. These measurements would have to be made well above balloon altitudes (> 50 km) to avoid significant atmospheric absorption of the x-rays.

R. A. Goldberg
S. A. Curtis
Laboratory for Planetary Atmospheres, NASA/Goddard Space Flight Center, Greenbelt, Maryland 20771
J. R. Barcus
Department of Physics, University of Denver, Denver, Colorado 80210
C. L. Siefring
M. C. Kelley
School of Electrical Engineering, Cornell University, Ithaca, New York 14853

References and Notes

1. R. A. Helliwell, *Space Sci. Rev.* **15**, 78 (1974).
2. C. G. Park and R. A. Helliwell, *Science* **200**, 727 (1978).
3. U. S. Inan, *Technical Report E477-1* (Radioscience Laboratory, Stanford University, Stanford, Calif., 1981).
4. ——, T. F. Bell, H. C. Chang, *J. Geophys. Res.* **87**, 6243 (1982).
5. R. M. Thorne and B. T. Tsurutani, *ibid.* **86**, 1639 (1981).
6. C. F. Kennel and H. E. Petschek, *ibid.* **71**, 1 (1966); L. R. Lyons, R. M. Thorne, C. F. Kennel, *ibid.* **77**, 3455 (1972); U. S. Inan, T. F. Bell, R. A. Helliwell, *ibid.* **83**, 3235 (1978); A. Tolstoy, T. J. Rosenberg, D. L. Carpenter, *Geophys. Res. Lett.* **9**, 563 (1982).
7. W. L. Imhof, R. R. Anderson, J. B. Reagan, E. E. Gaines, *J. Geophys. Res.* **86**, 11225 (1981).
8. U. S. Inan and R. A. Helliwell, *Geophys. Res. Lett.* **9**, 917 (1982).
9. H. C. Koons, B. C. Edgar, A. L. Vampola, *J. Geophys. Res.* **86**, 640 (1981).
10. T. J. Rosenberg *et al.*, *Eos* **63**, 408 (1982).
11. D. L. Carpenter and J. W. LaBelle, *J. Geophys. Res.* **87**, 4427 (1982).
12. E. A. Bering, T. J. Rosenberg, J. R. Benbrook, D. Detrick, D. L. Matthews, M. J. Rycroft, M. A. Sanders, W. R. Sheldon, *ibid.* **85**, 55 (1980); R. A. Helliwell and S. B. Mende, *ibid.*, p. 3376.

13. W. L. Imhof, J. B. Reagan, E. E. Gaines, R. A. Helliwell, U. S. Inan, J. P. Katsufrakis, R. G. Joiner, *Eos* **63**, 404 (1982).
14. W. L. Imhof, personal communication.
15. R. C. Davidson, *Methods in Nonlinear Plasma Theory* (Academic Press, New York, 1972), pp. 163–166.
16. M. J. Berger, S. M. Seltzer, K. Maeda, *J. Atmos. Terr. Phys.* **36**, 591 (1974).
17. M. C. Kelley *et al.*, *Eos* **62**, 988 (1981).
18. This experiment was made possible through the efforts of W. L. Imhof, who arranged coordination of the NSS transmitter with the rocket flights. We also thank P. Twigg for programming efforts, R. Hagemeyer and J. Modlin for flight and instrument engineering assistance, and M. Silbert, J. Brown, and L. Early for direction of the payload and flight support.

20 September 1982; revised 19 January 1983

Role of Surface-Active Phospholipids in Gastric Cytoprotection

Abstract. *Intragastric administration of a liposomal surfactant suspension markedly reduced acid-induced gastric ulcerogenesis and bleeding in rats. The concentration of surface-active molecules intrinsically present in the gastric mucosa was increased two to six times by administration of 16,16-dimethyl prostaglandin E_2. Thus, local accumulation of surface-active phospholipids may be an integral component of the cytoprotective mechanism activated by prostaglandin treatment.*

It is accepted that the amphoteric phospholipids secreted by alveolar type 2 cells are particularly active at the cell surface and play major roles in pulmonary mechanics and homeostasis (*1*). These phospholipids have been studied because of their ability to reduce surface tension at the interface between air and liquid (*1, 2*), but recently it was reported that the same class of surfactants can adsorb onto inert or biological membranes and enhance the hydrophobic properties of these surfaces (*3*). It is also recognized in the theory of corrosion inhibition that treatment of surfaces with cationic surfactants provides the underlying material with a hydrophobic coating that protects against hydrochloric acid and other noxious water-soluble agents in the environment (*4*).

Under normal conditions the mammalian gastric mucosa is protected from acid damage by a physicochemical barrier of unknown composition (*5, 6*). The integrity of this barrier may be compromised in patients who are predisposed to ulcer disease (*7*). Since surfactants may play a role in the maintenance of hydrophobic surfaces in the lung, it is possible that these substances have a similar function in the stomach. The gastric epithelium, like the pulmonary epithelium, has a highly hydrophobic surface with biophysical properties similar to those of polyethylene and other nonwettable substances (*8*). Several research groups including our own have identified surfactant compounds, previously thought to be unique to the lung, in both the gastric juice and mucosal surface of a variety of species including man (*9*). It is, therefore, of interest to investigate the role of extrinsic and intrinsic surface-active phospholipids in gastric cytoprotection.

Gastric necrosis and bleeding were induced in rats by a modification of the technique of Robert *et al.* (*10*). Fasted male rats were anesthetized with pentobarbital, the pylorus was ligated, and a cannula was positioned in the gastric lumen from an esophageal opening. The animals were then treated via the esophageal cannula with saline or a liposomal phospholipid suspension. The composition of phospholipids in the mixture was based on the concentration of these substances in pulmonary surfactant (*1*). Thirty minutes later an ulcerogenic dose of hydrochloric acid was administered by the same route. After 45 minutes the animals were killed and their stomachs were excised, opened along the greater curvature, and examined.

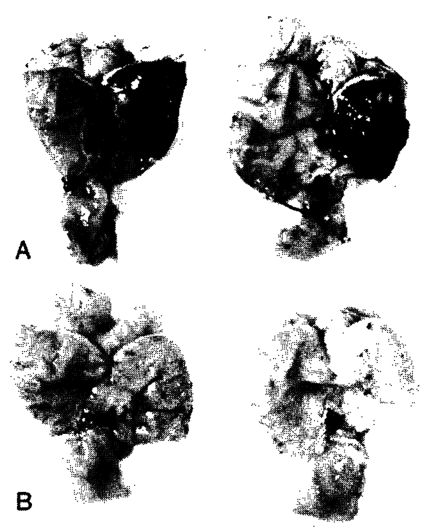

Fig. 1. Gross appearance of excised stomachs of pylorus-ligated rats treated with 1 ml of saline (A) or 1 ml of a surfactant mixture (B) 30 minutes before 1 ml of 0.6*M* HCl was administered intragastrically. The animals were killed 45 minutes after the acidic challenge. Stomachs were not heparinized when visually examined for ulcer formation. The surfactant mixture contained 135 μg of DP phosphatidylcholine and 15 μg of each of the following phospholipids: phosphatidylethanolamine, phosphatidylglycerol, phosphatidylinositol, and sphingomyelin. The organic solvent (ether) was removed by evaporation under N_2 and replaced with saline. A final aqueous liposomal suspension of the phospholipids was prepared by sonication of the mixture at 25°C for 1 minute. The suspension was stored at 4°C under N_2 until needed. In the controls the necrotic lesion formed only along the posterior wall of the stomach, where the acid pooled in the supine position.

Acid-induced gastric necrosis was markedly reduced by treatment with the surface-active phospholipids (Fig. 1). Surfactant administration did not provide protection by neutralization or dilution of the exogenous acid, since mean *p*H and volume of the gastric aspirates were virtually identical in the two groups (*p*H in control and surfactant-treated rats, 1.43 ± 0.03 and 1.41 ± 0.04, respectively; volume, 4.6 ± 0.2 and 4.3 ± 0.2 ml, respectively; $N = 5$ per group).

Intragastric bleeding in control and surfactant-treated rats was estimated by measuring the concentration of hemoglobin in heparinized gastric aspirates (*11, 12*). This technique was validated by demonstrating that the concentration of intragastric hemoglobin paralleled the release of ^{51}Cr-labeled red blood cells into the gastric juice in response to graded doses of exogenous HCl (0.15 to 0.6*M*) (Fig. 2A). Intragastric bleeding in surfactant-treated rats was 60 percent less than in controls (Fig. 2B).

Prostaglandins protect against gastric and duodenal ulcerogenesis and bleeding in both laboratory animals and man (*10, 13*). Evidence has also been obtained that prostaglandins are synthesized locally in the gastric mucosa and play a physiologically important role in protecting the tissue against damaging agents such as acid (*13*). It is, however, unclear how extrinsic or intrinsic prostaglandins exert their cytoprotective action. We therefore sought to determine (i) whether prostaglandins mediate protection induced by extrinsic phospholipids and (ii) whether the intrinsic phospholipids of the gastric mucosa mediate the cytoprotective mechanism initiated by the prostaglandins. The latter alternative seemed reasonable since prostaglandin treatment stimulates the secretion of surfactants by pulmonary alveolar cells (*14*).

The first possibility was investigated by treating rats with indomethacin, a selective inhibitor of prostaglandin synthesis (*15*), before the administration of the test agents. The dose of indomethacin employed was nonulcerogenic when administered alone but elicited marked aggravation of acid-induced bleeding (Fig. 2B). In addition, the phospholipid-induced reduction in gastrointestinal